Recent increase in summertime extreme wave heights in the western North Pacific

W. Sasaki, S. I. Iwasaki, T. Matsuura, and S. Iizuka

National Research Institute for Earth Science and Disaster Prevention, Tsukuba, Japan

Received 9 June 2005; revised 1 July 2005; accepted 18 July 2005; published 11 August 2005.

[1] Recent increase in summertime extreme wave heights (H_{10}, June–August average of the highest 10% of significant wave heights at each month) in the western North Pacific is found by applying an empirical orthogonal function analysis to H_{10} derived from 3rd–generation wave model forced by 6-hourly sea surface wind fields of NCEP-NCAR reanalysis over the period 1980–2004. The leading principal component of H_{10} demonstrates that the highest four years of H_{10} during 1980–2004 occurred in the last 10 years. It is found that the recent increase in H_{10} corresponds to the recent increase in total duration of intense tropical cyclones (ITC, with central pressure below 980 hPa) in the western North Pacific. Time series of the total duration of ITC reveals that the highest three years of the total duration of ITC during the last three decades occurred in the last 10 years. **Citation:** Sasaki, W., S. I. Iwasaki, T. Matsuura, and S. Iizuka (2005), Recent increase in summertime extreme wave heights in the western North Pacific, *Geophys. Res. Lett.*, *32*, L15607, doi:10.1029/2005GL023722.

1. Introduction

[2] Elucidating wave climate is of great importance for safe marine transport, offshore industries and the assessment of future vulnerability to coastal disaster. In addition, understanding the changes in wave climate gives a better understanding on the future wave climate in the greenhouse-gas-induced global warming. Although there have been many studies on the changes in the wintertime wave climate in the North Atlantic [*WASA group*, 1998; *Wang and Swail*, 2001] and the North Pacific [*Allan and Komar*, 2000; *Graham and Diaz*, 2001; *Wang and Swail*, 2001; *Hatada et al.*, 2001, 2002], the changes in the summertime wave climate have not been fully investigated. In the western North Pacific, the summertime wave climate is characterized by calm sea due to the moderate surface winds associated with the Pacific high and severe high waves caused by tropical cyclones (TCs). *Sasaki et al.* [2005] presented a study of interannual variability in wave data recorded at a site off the coast of southern Japan, and related an increased occurrence of waves of frequencies around 0.09 Hz with intense TC activity in the western North Pacific. It is important to clarify the changes in the summertime wave climate in the western North Pacific to also understand the changes in the TC activity.

[3] To investigate the long-term variability of ocean surface waves, reconstruction of wave histories by using numerical wave model could be the most effective method. Recently, wave reanalysis data covering the period 1957–2002 (ERA-40) has been made available by the European Centre for Medium-Range Weather Forecasts. The results of ERA-40 have been validated against observations [*Caires and Sterl*, 2005] and other reanalysis data sets [*Caires et al.*, 2004]. *Caires and Swail* [2004] represented, by using corrected significant wave heights (H_s) of ERA-40 (C-ERA-40, in which the inhomogeneity of 12/1991–05/1993 is not present), 40-yr (1958–2001) trends in the seasonal mean, 90th and 99th percentiles of H_s. They presented the 40-yr positive trend in the July–September mean, 90th and 99th percentiles of H_s in the western North Pacific.

[4] Our aim in this paper is to report and prove the increase in summertime extreme wave heights after the late 1990s in the western North Pacific. Three data sets are used: (1) Significant wave heights in ERA-40, (2) Wave data obtained by driving a numerical wave model. The sea surface wind fields used come from National Centers for Environmental Prediction–National Center for Atmospheric Research reanalysis (NRA) during 1980–2004, (3) The tropical cyclone data set. Although the extreme wave heights may be underestimated by coarse wind fields of NRA, which can not resolve tropical cyclones, we can discuss the qualitative remarks.

[5] This paper is arranged into four sections. In section 2, we introduce reanalysis data sets and define extreme wave heights. Numerical wave hindcast procedure is also described. Section 3 is devoted to the analysis of the increase in the extreme wave heights after the late 1990s in the western North Pacific. Section 4 gives summary and discussion.

2. Data and Model Description

2.1. Reanalysis and Observed Data Sets

[6] Significant wave heights of ERA-40 with 2.5° latitude-longitude grid during 1980–2002 is used in this study. The ERA-40 data have been obtained from the ECMWF data server. The data quality should be better for this period than for the earlier period, because satellite-derived information is available for the reanalysis scheme. Monthly extreme wave heights (MEWH) are defined as the average of the highest 10% of 6-hourly significant wave heights for each month. Extreme wave heights of ERA-40 for the summer mean (H_{10}^{ERA40}) are computed by averaging the MEWH for June–August. Although the significant wave heights of ERA-40 have high accuracy, there are inhomogeneities during December 1991 to May 1993 due to the assimilation of faulty ERS-1 FDP (Fast Delivery Product) [*Caires and Swail*, 2004] and the reanalysis period is somewhat short to depict the variability in H_{10} after the

0094-8276/05/2005GL023722$05.00

Table 1. Statistical Comparison of Hindcast Significant Wave Heights Versus in Situ Buoy Significant Wave Heights During 1980–2004

Buoy Number	Mean Error, m (Obs. Minus Model)	Root Mean Square Error, m	Corr. Coeff.
46001	0.40	1.20	0.71
46002	0.45	0.92	0.78
46005	0.40	1.03	0.77
46006	0.47	1.09	0.80

late 1990s. To extend the analysis period, we conduct wave hindcast by driving a wave model forced by sea surface wind fields of NRA. The wave model and hindcast procedure are described in the next subsection.

[7] To investigate the atmospheric-oceanic variation associated with the variation in H_{10}, we use sea surface wind fields of NRA [*Kalnay et al.*, 1996]. Monthly extreme wind speed (MEWS) is defined as the average of the highest 10% of the 6-hourly 10m sea surface wind speed for each month. Extreme wind speed for the summer mean (W_{10}) is computed by averaging the MEWS for June–August.

[8] We also employ observed TC data in the Typhoon Best-Track Data issued by the Regional Specialized Meteorological Center (RSMC) Tokyo Typhoon Center. The data provides basic information covering the TC's position, movement and intensity in the western North Pacific and the South China Sea. In this paper, we use the term TC to mean any of the following: a tropical storm (maximum sustained surface wind speeds between 17.3 ms^{-1} and 23 ms^{-1}), a severe tropical storm (23–32 ms^{-1}), or a typhoon (>33 ms^{-1}).

2.2. Numerical Wave Hindcast Procedure and Data Sets

[9] Numerical wave hindcast is performed by using the WAVEWATCH III model [*Tolman*, 2002], which is a full-spectral 3rd-generation wave model developed at National Oceanic and Atmospheric Administration–National Centers for Environmental Prediction. The model is configured at a spacing 0.75° latitude-longitude grid over the Pacific (75°S–75°N, 100°–295°E). Although the model domain has the closed boundary in the South Pacific, the swells which are formed in the South Indian Ocean and the South Atlantic Ocean would not strongly influence on the variation in significant wave heights in the western North Pacific. The wave spectrum is resolved into 24 directions and 23 frequencies. The directions begin at 0°N and span 360° clockwise in 15° increments. The frequencies begin with the lowest frequency at 0.04118 Hz and are logarithmically spaced with an increment factor of 1.1. The input wind fields are 10m sea surface winds of NRA with resolution 2.5° latitude-longitude grid. Approximately quadratic interpolation is used to generate new input wind fields to match the spatial resolution of the model. In the hindcast procedure, the input winds are updated at 6-hour intervals from 00Z01Nov1979 to 18Z31Aug2004. Output wave fields are archived at 6-hour intervals. The statistical comparison between the hindcast and observed significant wave heights in the eastern North Pacific is shown in Table 1. Although the hindcast significant wave heights have negative bias to the observed one, their correlation coefficients are high. Therefore, we conclude that we can use the hindcast results to investigate the changes in wave climate. Extreme wave heights for the summer mean (H_{10}) are computed by averaging the MEWH for June–August.

3. Results

3.1. Increase in H_{10}^{ERA40} and H_{10} in the Western North Pacific

[10] Our main analysis domain is limited within the western North Pacific (0°–40°N, 100°–180°E), since the standard deviation of H_{10}^{ERA40} during 1980–2002 is markedly large over the region (figure is not shown). To identify the most prevailing spatial and temporal variation in H_{10}^{ERA40} within the analysis domain, we applied an empirical orthogonal function (EOF) analysis to H_{10}^{ERA40} during 1980–2002. The first EOF accounts for 52.5% of the covariance matrix variance within the analysis domain. The explained variance of the 2nd and 3rd modes are 11.7% and 5.7%, respectively. From the small difference in the explained variance between the 2nd and 3rd modes, we conclude that only the first mode is meaningful. The first mode of EOF represents the anomalies of H_{10}^{ERA40} in the western North Pacific (Figure 1a). In particular, the anomalies of H_{10}^{ERA40} in the south of Japan (10°–30°N, 120°–150°E) are markedly large. The time series of the leading principal component

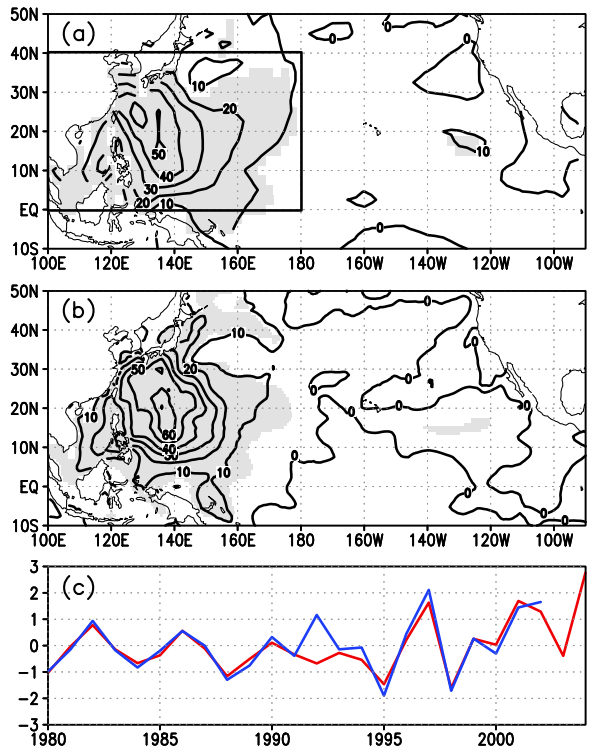

Figure 1. (a) The first EOF mode of H_{10}^{ERA40} in the western North Pacific. The domain for our EOF analysis is bounded by bold lines (0°–40°N, 100°–180°E). Contour shows the linear regression coefficient between H_{10}^{ERA40} and the time series of the leading principal component (PC1) shown in Figure 1c. Shaded grid shows where the local correlation between the PC1 and H_{10}^{ERA40} is statistically significant at 1% level (results of t-test). (b) As in Figure 1a, but for H_{10} instead of H_{10}^{ERA40}. (c) Normalized time series of PC1 of H_{10}^{ERA40} (blue line) and H_{10} (red line).

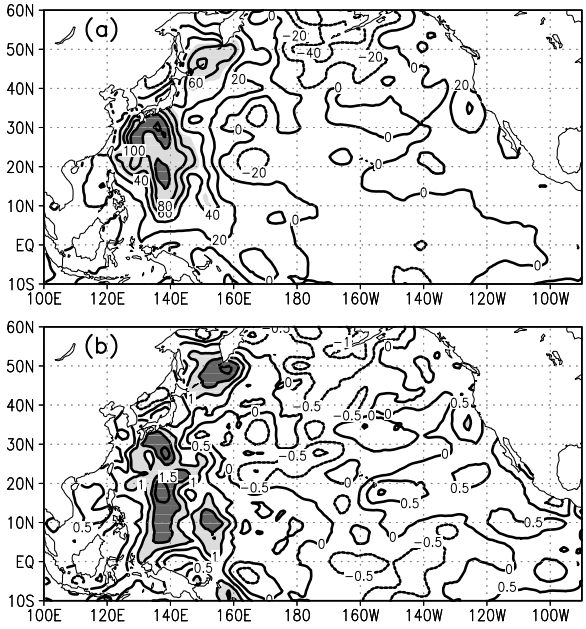

Figure 2. (a) The difference in H_{10} (cm) between the early and later years (the later years minus the early years). Contour intervals are 20. Grid shaded heavily and lightly indicates where the difference exceeds 100 and 50, respectively. (b) As in Figure 2a, but for W_{10} instead of H_{10}. Unit is ms^{-1}. Grid shaded heavily and lightly indicates where the difference exceeds 1.5 and 1.0, respectively.

(PC1) shows the interannual variability and the frequent occurrences of higher positive anomalies after the late 1990s (Figure 1c). The positive anomalies in the PC1 in 1982, 1986, 1997 and 2002 correspond to the ENSO years. The interannual variability of the summertime significant wave heights in the western North Pacific is affected by TC activity associated with the ENSO event (W. Sasaki et al., manuscript in preparation). To extend the analysis period after the late 1990s, an EOF analysis is also applied to H_{10} during 1980–2004. The first EOF mode of H_{10}, which accounts for 56.4% of the total variance, shows spatial and temporal variations similar to those of H_{10}^{ERA40} (Figures 1a–1c). Some differences in the related first EOF may be attributed to the difference in the variance between H_{10} and H_{10}^{ERA40}. Time series of the PC1 of H_{10} coincides with that of H_{10}^{ERA40} except in 1992. This gap could be due to the inhomogeneity in significant wave heights of ERA-40 aforementioned. In this paper, we focus on the increasing frequency of higher H_{10} after the late 1990s, which are due to the large positive anomalies in 1997, 2001, 2002 and 2004 (Figure 1c). It is striking that the highest four years of H_{10} during 1980–2004 occurred in the last 10 years. Figure 2a shows the difference in H_{10} between two sets of four summers (i.e., 1982, 1986, 1990 and 1996; and 1997, 2001, 2002 and 2004) during which PC1 was positive during 1980–1996 and 1997–2004, respectively. We call the former and latter sets of summers 'early years' and 'later years', respectively. The difference in H_{10} between the early and later years is larger than 50 cm in the south of Japan and east of the Sea of Okhotsk (Figure 2a). In particular, the difference within the region 25°–35°N, 130°–140°E and 15°–20°N, 135°–140°E is over 1 m. It is found that the area where the difference in W_{10} is large (0°–35°N, 130°–140°E) corresponds to the area where H_{10} have large differences (Figures 2a and 2b). This result supports the increase in H_{10} after the late 1990s. In the next subsection we examine, by using observational TC data, the recent increase in H_{10} after the late 1990s in the western North Pacific.

3.2. Increase in Total Duration of Intense Tropical Cyclone

[11] Figure 3a shows the latitudinal distribution of TC's central pressure averaged for the longitudinal band 120°–150°E. The TC's central pressure in the early years is 5–10 hPa stronger than that averaged for 1980–2004 within the latitudinal range 20°–25°N (dotted and dashed lines in Figure 3a). This result supports that H_{10} in the early years are higher than the average. The TC's central pressure in the later years is more than 5 hPa stronger than that in the early years within the latitudinal range 15°–30°N (solid and dotted line in Figure 3a). Although the TC's central pressure at 24°N is stronger in the early years than in the later years, the TC's central pressure in the later years is stronger than in the early years within most of the latitudinal band 10°–30°N. The latitudinal band 15°–30°N of the large difference in TC's central pressure corresponds to the region where H_{10} and W_{10} have large difference (Figures 2a and 2b).

[12] Changes in the summertime wave climate at a site off the coast of southern Japan are related to intense tropical cyclone (with central pressure below 980 hPa, ITC) activity [*Sasaki et al.*, 2005]. Therefore, the ITC activity is a key to

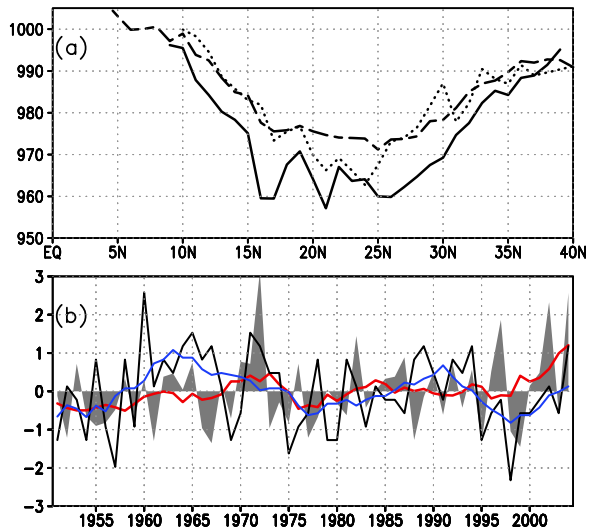

Figure 3. (a) Latitudinal distribution of TC's central pressure (hPa) averaged for the longitudinal band 120°–150°E. Solid and dotted line shows the mean central pressure of TC in the later and early years, respectively. Dashed line shows the mean central pressure of TC during 1980–2004. (b) Normalized time series of the total duration (hour) of ITC within the region 0°–35°N, 120°–160°E during June–August (shaded) and the frequency of TC which passed within the region 0°–35°N, 120°–160°E during June–August (solid line). Red and blue lines show the total duration of ITC and the frequency of TC smoothed by means of a 5–year moving average, respectively.

understanding the summertime wave climate in the western North Pacific. We now focus on the duration of ITC. The total duration of ITC is defined as the sum of the duration of each ITC within the region 0°–35°N, 120°–160°E during June–August. The total duration of ITC has the high peak in the early 1970s, low peak in the late 1970s, high peak in the mid 1980s and rapid increase after the late 1990s (red line in Figure 3b). The rapid increase after the late 1990s is due to the highest three years of 1997, 2002 and 2004 since 1973. The years 1997, 2002 and 2004 corresponds to high H_{10} years since 1980. Correlation coefficient between PC1 for H_{10} and the total duration of ITC is statistically significant at 1% level ($r = 0.77$). A remarkable feature in the time series of the total duration of ITC is that the total duration of ITC after the late 1990s is the highest in the last three-decades, and the highest three years occurred in the last 10 years.

[13] In contrast, the frequency of TC can not explain adequately the recent increase in H_{10}. The frequency recordings of TC, defined as the number of TC which passed within the region 0°–30°N, 120°–160°E during June–August, show positive anomalies during 1988–1994 and negative anomalies after 1995 (Figure 3b). On the other hand, it is obvious that the total duration of ITC shows positive anomalies after 1995. Correlation coefficients between PC1 for H_{10} and the frequency of TC is not statistically significant at 1% level ($r = 0.33$). As a result, we can conclude that the recent increase in the summertime H_{10} in the western North Pacific is due to the increase in the total duration of ITC after the late 1990s.

4. Summary and Discussion

[14] In this study, we have shown, by analyzing the interannual variability of H_{10} in the western North Pacific, that the highest four years of H_{10} during 1980–2004 occurred in the last 10 years, and related the recent increase in H_{10} with the recent increase in the total duration of ITC in the western North Pacific.

[15] SST may be a possible cause of the increase in the duration of ITC, since warm SST is favorable for the intensification of TC [*Evans*, 1993; *Kuroda et al.*, 1998]. Significant differences in SST between the early and later years are observed in the western North Pacific (figure is not shown). This region corresponds to the region where the TC's central pressure is lower in the later years than in the early years (Figure 3a). Warmer SST within the region may intensify TCs and sustain the TC's intensity.

[16] *Meehl et al.* [2000] documented that the increase in TC intensity and decrease in TC frequency in the greenhouse gas–induced climate warming by driving the high resolution ocean-atmosphere coupled model. *Wang and Swail* [2004] showed that significant changes in seasonal (July–September) extreme significant wave heights can be anticipated around southern Japan in the western North Pacific by using projections of future climate conducted with three coupled Atmosphere-Ocean General Circulation Models. Though we can not determine that the recent increase in H_{10} and TC intensity is due to the influence of the global warming, it is striking that the relationship between the rise in SST and the increase in H_{10} was found in the present analysis. We need further investigation on the relationship between the variation in SST and the TC activity, which strongly affects the changes in the wave climate in the western North Pacific.

References

Allan, J. C., and P. D. Komar (2000), Are ocean wave heights increasing in the eastern North Pacific?, *Eos Trans. AGU*, *47*, 561–567.

Caires, S., and A. Sterl (2005), A new non-parametric method to correct model data: Application to significant wave height from the ERA-40 reanalysis, *J. Atmos. Oceanic Technol.*, *22*, 443–459.

Caires, S., and V. R. Swail (2004), Global wave climate trend and variability analysis, paper presented at 8th International Workshop on Wave Hindcasting and Forecasting, North Shore, Hawaii.

Caires, S., A. Sterl, J. R. Bidlot, N. Graham, and V. R. Swail (2004), Intercomparison of different wind wave reanalysis, *J. Clim.*, *17*, 1893–1913.

Evans, J. L. (1993), Sensitivity of tropical cyclone intensity to sea surface temperature, *J. Clim.*, *6*, 1133–1140.

Graham, N. E., and H. F. Diaz (2001), Evidence for intensification of North Pacific winter cyclones since 1948, *Bull. Am. Meteorol. Soc.*, *82*, 1869–1893.

Hatada, Y., M. Yamaguchi, M. Ohfuku, M. J. Li, and H. Nonaka (2001), Applicability of a 20-year wave hindcast system to the wave etimation on coastal area of Japan (in Japanese), *J. Jpn. Soc. Nat. Disaster Sci.*, *20*, 307–324.

Hatada, Y., M. Yamaguchi, M. Ohfuku, M. J. Li, and H. Nonaka (2002), Estimation of long term variability of wave height climate around the coastal sea areas of Japan (in Japanese), *Annu. J. Eng. Ehime Univ.*, *1*, 217–229.

Kalnay, E., et al. (1996), The NCEP/NCAR 40-yr reanalysis project, *Bull. Am. Meteorol. Soc.*, *77*, 437–471.

Kuroda, M., A. Harada, and K. Tomine (1998), Some aspects on sensitivity of typhoon intensity to sea surface temperature, *J. Meteorol. Soc. Jpn.*, *76*, 1145–1151.

Meehl, G. A., F. Zwiers, J. Evans, T. Knutson, L. Mearns, and P. Whetton (2000), Trends in extreme weather and climate events: Issues related to modeling extremes in projections of future climate change, *Bull. Am. Meteorol. Soc.*, *81*, 427–436.

Sasaki, W., S. I. Iwasaki, T. Matsuura, S. Iizuka, and I. Watabe (2005), Changes in wave climate off Hiratsuka, Japan, as affected by storm activity over the western North Pacific, *J. Geophys. Res.*, doi:10.1029/2004JC002730, in press.

Tolman, H. L. (2002), User manual and system documentation of WAVEWATCH-III version 2.22, *NOAA/NWS/NCEP/MMAB Tech. Note 222*, Natl. Oceanic and Atmos. Admin., Silver Spring, Md.

Wang, X. L., and V. R. Swail (2001), Changes of extreme wave heights in Northern Hemisphere oceans and related atmospheric circulation regimes, *J. Clim.*, *14*, 2204–2221.

Wang, X. L., and V. R. Swail (2004), Projections of ocean wave heights—Climate change signal and uncertainty, paper presented at 8th International Workshop on Wave Hindcasting and Forecasting, North Shore, Hawaii.

WASA Group (1998), Changing waves and storms in the northeast Atlantic?, *Bull. Am. Meteorol. Soc.*, *79*, 741–760.

S. Iizuka, S. I. Iwasaki, T. Matsuura, and W. Sasaki, National Research Institute for Earth Science and Disaster Prevention, 3-1 Tennoudai, Tsukuba 305-0006, Japan. (wsasaki@bosai.go.jp)